Inorg. Chem. **2006**, *45*, 9475–9479

Synthesis and Magnetic Properties of an Amine-Templated Fe^{2+} ($S = 2$) Sulfate with a Distorted Kagome Structure

J. N. Behera and C. N. R. Rao*

Chemistry and Physics of Materials Unit, Jawaharlal Nehru Centre for Advanced Scientific Research, Jakkur P. O., Bangalore 560064, India, and Solid State and Structural Chemistry Unit, Indian Institute of Science, Bangalore 560012, India

Received August 3, 2006

An organically templated iron(II) sulfate of the composition $[H_3N(CH_2)_2NH_2(CH_2)_2(NH_3]_4[Fe^{II}_9F_{18}(SO_4)_6]\cdot 9H_2O$ with a distorted Kagome structure has been synthesized under solvothermal conditions in the presence of diethylenetriamine. The distortion of the hexagonal bronze structure comes from the presence of two different types of connectivity between the FeF_4O_2 octahedra and the sulfate tetrahedra. This compound exhibits magnetic properties different from those of an Fe(II) compound with a perfect Kagome structure and is a canted antiferromagnet at low temperatures.

Introduction

Transition metal compounds with the Kagome structure have been investigated extensively because of their interesting magnetic properties. The literature abounds with studies of Kagome compounds of Fe^{3+}($S = 5/2$), such as the family of jarosites, all of which exhibit magnetic frustration or low-temperature antiferromagnetism.[1] Most of the Fe^{3+} jarosites investigated are not pure because of the presence of site defects. It is only recently that Nocera et al.[2,3] prepared a pure Fe^{3+} jarosite by redox-based hydrothermal methods. In this compound, the Fe^{3+} Kagome layer shows an antiferromagnetic transition at 61.4 K. A pure $S = 1/2$ copper Kagome compound has been found to show spin frustration,[4] while a Co^{2+} ($S = 3/2$) compound shows properties similar to those of the Fe^{3+} jarosites.[5] On the other hand, V^{3+} ($S = 1$) Kagome compounds exhibit ferromagnetic coupling within the triangles of Kagome layer.[6] Ferromagnetic interactions are also found in Fe^{2+} ($S = 2$) Kagome compounds.[7] A recent study of a Ni^{2+} ($S = 1$) Kagome compound has shown it to be a canted antiferromagnet.[8] The Fe^{2+} Kagome compounds investigated hitherto are $[H_3N(CH_2)_6NH_3][Fe^{II}_{1.5}F_3(SO_4)]\cdot 0.5H_2O$, **I**,[7a] and $[H_3N(CH_2)_2NH_2(CH_2)_2NH_2(CH_2)_2NH_3][Fe^{II}_3F_6(SO_4)_2]$, **II**.[7b] **I** has a perfect Kagome structure with uniform hexagonal bronze layers, and **II** has a slightly distorted structure. A significant question in this context concerns the relationship between the distortion of the hexagonal layers and the magnetic properties of the Kagome compounds. We have now prepared a compound of the formula $[H_3N(CH_2)_2NH_2(CH_2)_2NH_3]_4[Fe^{II}_9F_{18}(SO_4)_6]\cdot 9H_2O$, **III**, which is highly distorted compared to **I** and **II** and shows different magnetic properties. We describe the structure and properties of **III** in this article.

Experimental Section

Synthesis and Characterization. In a typical synthesis of $[H_3N(CH_2)_2NH_2(CH_2)_2NH_3]_4[Fe^{II}_9F_{18}(SO_4)_6]\cdot 9H_2O$, **III**, 0.263 g of iron(III) citrate was dispersed in an ethanol (EtOH)−water mixture (5.8 and 1.8 mL, respectively) under constant stirring. To this mixture, 0.22 mL of sulfuric acid (98%) and 0.38 mL of diethyl-

* To whom correspondence should be addressed. E-mail: cnrrao@jncasr.ac.in. Fax: +91-80-2208-2760.

(1) (a) Ramirez, A. P. *Annu. Rev. Mater. Sci.* **1994**, *24*, 453. (b) Greedan, J. E. *J. Mater. Chem.* **2001**, *11*, 37. (c) Nocera, D. G.; Bartlett, B. M.; Grohol, D.; Papoutsakis, D.; Shores, M. P. *Chem.—Eur. J.* **2004**, *10*, 3850. (d) Wills, A. S.; Harrison, A.; Ritter, C.; Smith, R. I. *Phys. Rev. B* **2000**, *61*, 6156. (e) Wills, A. S.; Harrison, A. *J. Chem. Soc., Faraday Trans.* **1996**, *92*, 2161.
(2) Bartlett, B. M.; Nocera, D. G. *J. Am. Chem. Soc.* **2005**, *127*, 8985.
(3) Grohol, D.; Nocera, D. G.; Papoutsakis, D. *Phys. Rev. B* **2003**, *67*, 064401.
(4) Shores, M. P.; Nytko, E. A.; Bartlett, B. M.; Nocera, D. G. *J. Am. Chem. Soc.* **2005**, *127*, 13462.
(5) Behera, J. N.; Paul, G.; Choudhury, A.; Rao, C. N. R. *Chem. Commun.* **2004**, 456.
(6) (a) Grohol, D.; Papoutsakis, D.; Nocera, D. G. *Angew. Chem., Int. Ed.* **2001**, *40*, 1519. (b) Grohol, D.; Huang, Q.; Toby, B. H.; Lynn, J. W.; Lee, Y. S.; Nocera, D. G. *Phys. Rev. B* **2003**, *68*, 094404. (c) Papoutsakis, D.; Grohol, D.; Nocera, D. G. *J. Am. Chem. Soc.* **2002**, *124*, 2647.
(7) (a) Rao, C. N. R.; Sampathkumaran, E. V.; Nagarajan, R.; Paul, G.; Behera, J. N.; Choudhury, A. *Chem. Mater.* **2004**, *16*, 1441. (b) Paul, G.; Choudhury, A.; Rao, C. N. R. *Chem. Commun.* **2002**, 1904.
(8) Behera, J. N.; Rao, C. N. R. *J. Am. Chem. Soc.* **2006**, *128*, 9334.

10.1021/ic061457y CCC: $33.50
Published on Web 10/13/2006

enetriamine (DETA, 99.98%) were added, followed by the addition of 0.36 mL of HF (40%). The resultant mixture with the molar composition of iron(III) citrate/4H_2SO_4/3.5DETA/100EtOH/100H_2O/8HF had an initial pH of 4 after it had been stirred for 2 h. The mixture was taken in a 23 mL PTFE-lined acid-digestion bomb and heated at 180 °C for 4 days. After it was cooled to room temperature, the product containing thin plate-shaped crystals of **III** (yield 30% with respect to Fe) was filtered and washed with water and then with ethanol.

The initial characterization of **III** was carried out by powder X-ray diffraction (PXRD), energy-dispersive analysis of X-rays (EDAX), thermogravimetric analysis (TGA), and IR spectroscopy. Magnetic measurements on powdered samples were performed at temperatures between 2 and 300 K, in a vibrating sample magnetometer using a physical property measurement system (quantum design). PXRD patterns indicated the products to be new materials and monophasic, the patterns being consistent with those generated from single crystal X-ray diffraction. EDAX gave the expected metal/sulfate ratio of 3:2. The fluoride test was performed qualitatively, and quantitative analysis was performed by field emission scanning electron microscopy (FE-SEM). Bond valence sum calculations and the absence of electron density near fluorine in the difference Fourier map also provide evidence for the presence of fluorine. The water content of **III** was established by thermogravimetric analysis (TGA) to be close to the value given by the formula.

The infrared spectrum of **III** showed characteristic bands in the 980−1010 cm^{-1} region from ν_1 and in the 1090−1140 cm^{-1} region from ν_3 of SO_4^{2-}. The bending mode of SO_4^{2-} was in the 450−600 cm^{-1} region. The stretching and bending modes of the NH_2/NH_3^+ groups and H_2O were also in the expected ranges.[9]

Single-Crystal Structure Determination. A suitable single crystal of compound **III** was carefully selected under a polarizing microscope and mounted at the tip of the thin glass fiber using cyanoacrylate adhesive. The single-crystal structure determination by X-ray diffraction was performed on a Siemens SMART-CCD diffractometer equipped with a normal focus, 2.4 kW sealed-tube X-ray source (Mo Kα radiation, $\lambda = 0.71073$ Å) operating at 40 kV and 40 mA. The structure was solved by direct methods using SHELXS-97,[10] which readily revealed all the heavy-atom positions (Fe and S) and allowed us to locate the other non-hydrogen (C, N, O, and F) positions from the difference Fourier maps. An empirical absorption correction based on symmetry-equivalent reflections was applied using SADABS.[11] All the hydrogen positions were found in the difference Fourier maps. For the final refinement, the hydrogen atoms of the amine were placed geometrically and held in the riding mode. The last cycles of refinement included atomic positions, anisotropic thermal parameters for all the non-hydrogen atoms, and isotropic thermal parameters for hydrogen atoms of the amine. The hydrogen positions for water molecules were excluded from the final refinement. Full -matrix least-squares structure refinement against $|F^2|$ was carried out using the SHELXL-97[12] package of programs. Details of the structure determination and final refinements for **III** are listed in Table 1. The positions of the fluorine atoms in **III** were located primarily by examination of their thermal parameters. Their assignment as oxygen instead of fluorine invariably leads to nonpositive definite values when they were refined with anisotropic displacement parameters. The powder X-ray diffraction pattern of **III** was in good agreement with the simulated pattern based on the single-crystal data, indicative of phase purity.

Table 1. Crystal Data and Structure Refinement Parameters for **III**

empirical formula	$C_{16}H_{82}F_{18}N_{12}O_{33}S_6FeII_9$
formula mass	2008.01
cryst syst	triclinic
space group	$P\bar{1}(2)$
a (Å)	11.0438(2)
b (Å)	15.8352(2)
c (Å)	19.5662(4)
α (deg)	77.4810(10)
β (deg)	74.2310(10)
γ (deg)	71.1710(10)
vol (Å^3)	3085.31(10)
Z	2
T (°C)	20
ρ_{calcd} (g cm^{-3})	2.161
λ(Mo Kα) (Å)	0.71073
μ (mm^{-1})	2.403
θ range (deg)	1.09−23.24
total data collected	8682
R_{int}	0.0475
R [$I > 2\sigma(I)$]	R1 = 0.0642[a], wR2 = 0.1766[b]
R (all data)	R1 = 0.112, wR2 = 0.2129
GOF (S)	0.906

[a] $R1 = \sum|F_0| - |F_c|/\sum|F_0|$. [b] $wR2 = \{[w(F_0^2 - F_c^2)^2]/[w(F_0^2)^2]\}^{1/2}$, $w = 1/[\sigma^2(F_0)^2 + (aP)^2 + bP]$, $P = [F_0^2 + 2F_c^2]/3$, where $a = 0.1302$ and $b = 0$.

Results and Discussion

$[H_3N(CH_2)_2NH_2(CH_2)_2NH_3]_4[Fe^{II}_9F_{18}(SO_4)_6]\cdot 9H_2O$, **III**, has an asymmetric unit with 85 non-hydrogen atoms, of which 58 belong to the inorganic framework and 37 belong to the extraframework including nine water molecules (Figure 1a). There are 10 crystallographically distinct Fe atoms and six S atoms with all the Fe atoms in octahedral geometry. The Fe atoms have fluorine and oxygen neighbors to form FeF_4O_2 octahedra. There are two types of octahedral arrangements around the metal ion. In one, four F atoms are in equatorial positions, and two O are in the axial position as in jarosites; the other type has three F and one O in equatorial positions and one F and one O in axial positions (Figure 1b). Anionic layers of vertex-sharing $Fe^{II}F_4O_2$ octahedra and SO_4 tetrahedra are linked by Fe−F−Fe and Fe−O−S bonds. Note that in the perfect Kagome lattice of **I**, the six coordination of the metal ion is satisfied by the presence of four F atoms in equatorial positions, with the two axial positions occupied by the oxygen atoms of the sulfate (Figure 1c). As a result of the two types of Fe octahedra, the hexagonal structure of **III** gets distorted from that of a perfect Kagome lattice. Because 33% of the sulfate tetrahedra share equitorial oxygen with the iron octahedra, they do not lie perfectly on the triangular lattice and, instead, get tilted. The bridging fluorines connect Fe(II) ions with an Fe−F−Fe angle of 124.6−132.7° to form a triangular μ-fluoro trimer, which is capped by the sulfate anion. Because of the presence of F and O in both axial and equatorial positions of the octahedra, two types of triangular lattices are created, and the structure

(9) Nakamoto, K. *Infrared and Raman Spectra of Inorganic and Coordination Compounds*; Wiley-Interscience, New York, 1978.
(10) Sheldrick, G. M. *SHELXS-97, Program for Crystal Structure Determination*; University of Göttingen: Göttingen, Germany, 1997. (b) Sheldrick, G. M. *Acta Crystallogr., Sect. A* **1990**, *46*, 467.
(11) Sheldrick, G. M. *SADABS*: *Siemens Area Detector Absorption Correction Program*; University of Göttingen: Göttingen, Germany, 1994.
(12) Sheldrick, G. M. *SHELXTL-PLUS, Program for Crystal Structure Solution and Refinement*; University of Göttingen: Göttingen, Germany, 1997.

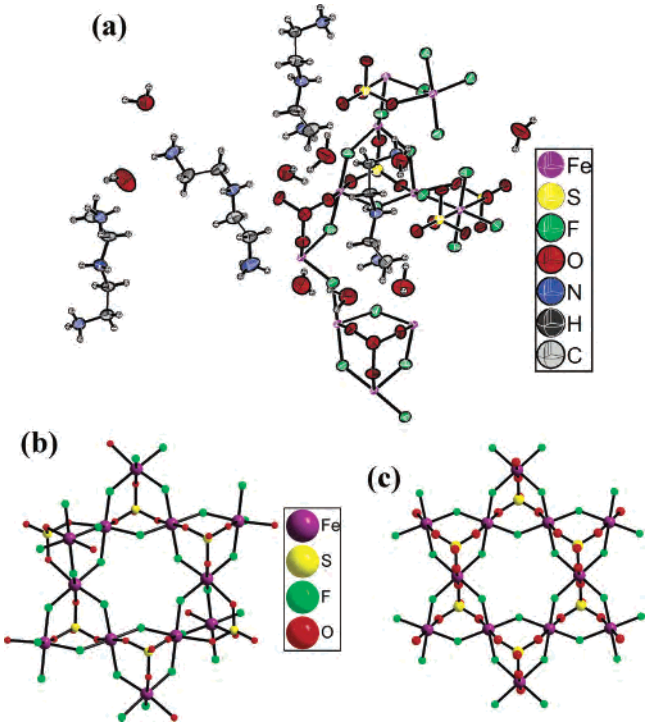

Figure 1. (a) ORTEP plot of $[C_{16}N_{12}H_{64}][Fe^{II}_9F_{18}(SO_4)_6]0{\cdot}9H_2O$, **III**. Thermal ellipsoids are given at 50% probability. The connectivity of the iron octahedra and the sulfate tetrahedra in **III** and in the perfect Kagome structure of **I** are shown in panels b and c, respectively.

gets distorted from the normal Kagome lattice. One type of three-ring trio is formed by the vertex-sharing of the FeF_4O_2 octahedra creating a perfect three-membered ring which is capped by the sulfate tetrahedron as in jarosites. On the other hand, the three-ring trio formed by the sharing of an equatorial corner between two octahedra and the axial corners shared with two equatorial positions a third octahedron gives rise to a distorted triangular unit. The presence of both perfect and distorted triangular units gives rise to symmetric and unsymmetric hexagons in **III**.

The Fe−O bond distances in **III** are in the range of 2.127(5)−2.176(5) Å with $(Fe-O)_{av}$ = 2.158 Å. The Fe−F bond distances are in the range of 2.008(4)−2.119(4) Å with $(Fe-F)_{av}$ = 2.068 Å. Bond valence calculations[13] using r_0(Fe−F) = 1.65 Å and r_0(Fe−O) = 1.734 Å (Fe(1) = 1.96, Fe(2) = 1.97, Fe(3) = 1.98, Fe(4) = 1.89, Fe(5) = 1.98, Fe(6) = 1.90, Fe(7) = 1.85, Fe(8) = 1.96, Fe(9) = 1.91, and Fe(10) = 1.93) and the average bond distance value indicate that the valence state of all the iron atoms is +2. The bond lengths and angles are in good agreement with those reported for the Fe^{2+} in fluorine and oxygen environments.[7] The Mössbauer spectrum shows the presence of the characteristic signal from Fe^{2+}. The position of fluorine atoms is supported by the calculated bond valence sums which lie in the 0.64−0.72 range. The framework stoichiometry of $[Fe^{II}_9F_{18}(SO_4)_6]$ with a −12 charge is balanced by the presence of triprotonated DETA molecules residing in the crest and trough regions of the corrugated layers and in the interlayer space where water molecules are also present

(13) Brown, I. D.; Altermatt, D. *Acta Crystallogr., Sect. B* **1985**, *47*, 244.

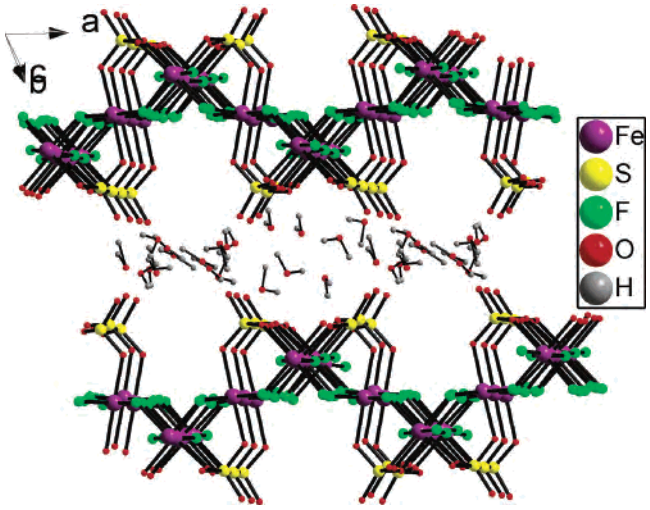

Figure 2. View down the *c* axis showing the stacking of the layers in **III**. DETA molecules are not shown in the interlayer space for purpose of clarity.

(Figure 2). The layers in **III** are stacked along the *b* axis in an ABAB fashion and are held together by hydrogen bonding interactions with the triprotonated amine and water molecules.

In Figure 3, we compare the structure of **III** with that of the perfect Kagome structure of **I** and the slightly distorted structure of **II**. Note that **I** contains only vertex-shared octahedra and, hence, symmetrical hexagons characteristic of the tungsten bronze layer (Figure 3a).[14] In **II**, the distorted structure results from the edge sharing of octahedra with two types of triangular units (Figure 3b). We realized that the distortion in **III** (Figure 3c) is far greater than that in **II**.

The TGA curve of **III** (N_2 atmosphere, range of 30−900 °C, heating rate 5 °C/min, given as Supporting Information) showed weight losses in three steps. The first weight loss corresponds to the loss of guest water molecules in the 60−200 °C range [obsd = 7.8%, calcd = 8%]; the major weight loss in the 200−400 °C range corresponds to the loss of amine and HF [obsd = 30.6%, calcd = 31.8%]. The third weight loss in the region of 400−800 °C corresponds to the removal of fluorine and the decompositions of sulfate [obsd = 27%, calcd = 25%]. The sample heated at 900 °C diffracts weakly, and the PXRD corresponds mixture of Fe_2O_3 and FeO (JCPDS files 00-003-0800 and 00-002-1186, respectively).

The magnetic properties of the jarosites are known to be sample dependent.[1d,1e] It is expected that any small perturbation would have a strong effect on the ground-state manifold. In Figure 4, we present the magnetic data on **III**. From the high-temperature inverse-susceptibility data of **III,** recorded at 1000 Oe (see inset a of Figure 4), we estimate a Weiss temperature of −105 K (θ_p), suggesting dominant antiferromagnetic exchange interactions. The effective magnetic moment per iron atom is 5.02 μ_B, which is close to the spin-only (S = 2) value of 4.9 μ_B for Fe^{2+} and is comparable to the values reported for similar compounds.[15] Furthermore,

(14) Magneli, A. *Acta Chem. Scand.* **1953**, *7*, 315.
(15) (a) Paul, G.; Choudhury, A.; Rao, C. N. R. *Chem. Mater.* **2003**, *15*, 1174. (b) Fu, A.; Huang, X.; Li, J.; Yuen, T.; Lin, C. L. *Chem.—Eur. J.* **2002**, *8*, 2239.

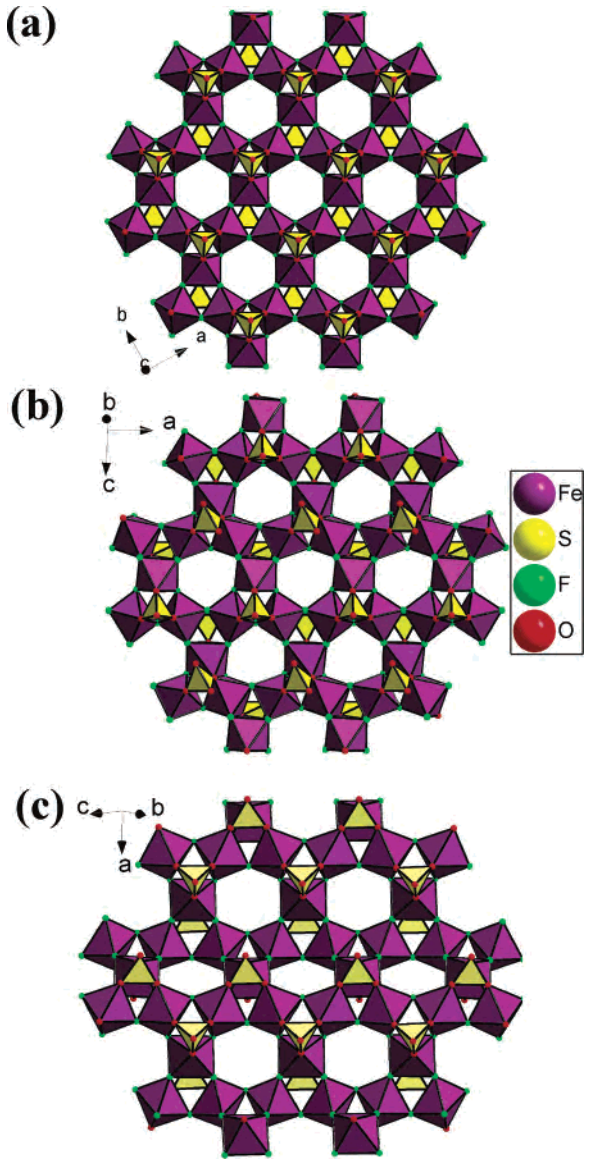

Figure 3. Polyhedral views of the hexagonal Kagome layers in **I**, **II**, and **III** are shown in panels a, b, and c, respectively. Notice how c has the most distorted structure and a has the perfect structure.

III shows magnetic hysteresis at low temperatures (inset b of Figure 4). The magnetization increases with the field without any evidence for saturation, implying an antiferromagnetic component as well, in agreement with the negative θ_p. The magnetic behavior of **III** is quite different from that of **I** or **II**. In Figure 5a and b, we compare the magnetic susceptibilities of **I**, **II,** and **III** measured at 100 Oe under field-cooled (FC) and zero-field-cooled (ZFC) conditions. Particularly important is the fact that magnetic susceptibility of this distorted compound (**III**) is very different from the previous compounds (**I** and **II**), mainly in the intermediate temperature regime, down to very low temperature. The broad nature of the ZFC susceptibility around $T \approx 10$ K suggests magnetic polarizations caused by some interactions, the strength of which is in the intermediate energy scale (kT $\approx$ 10 K). Since this appears in a distorted system, the magnetic polarizations must have a geometrical origin. It is by now quite well-known that distortions in a corner shared

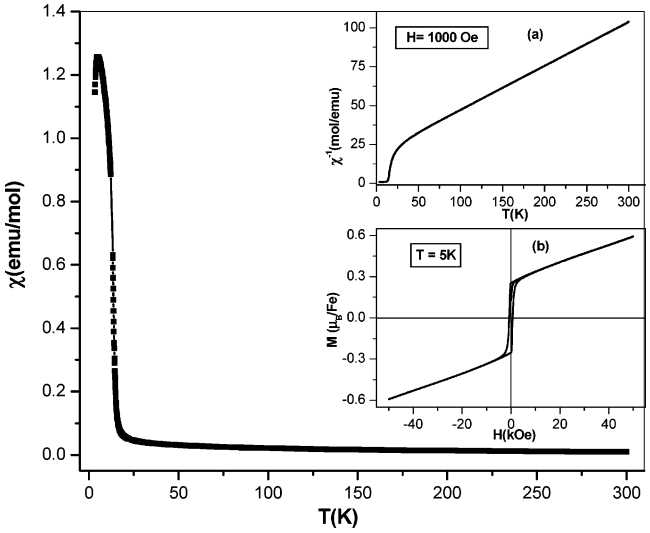

Figure 4. Temperature dependence of the magnetic susceptibility of **III** at 1000 Oe. Inset a shows the temperature variation of the inverse susceptibility at 1000 Oe. Inset b shows magnetic hysteresis at 5 K.

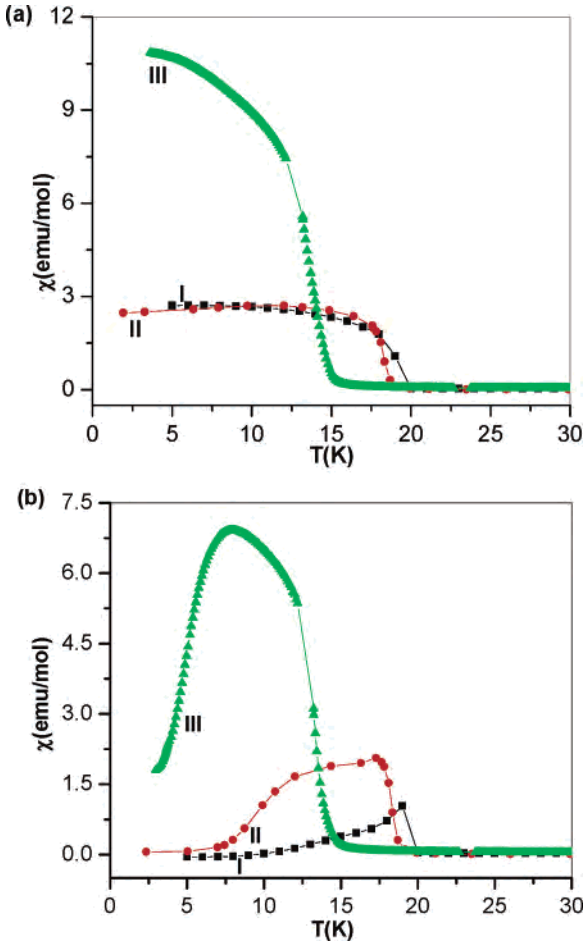

Figure 5. Comparison of the magnetic susceptibility data of **III** at 100 Oe with **I** and **II** under (a) field-cooled (FC) and (b) zero-field-cooled (ZFC) conditions.

Kagome lattice leads to Dzyaloshinsky−Moriya (DM) interactions, the in-plane components of which can give rise to magnetic polarizations in the out-of-plane directions with canted vectors of magnetic moments.[16] It is interesting to

(16) Elhajal, M.; Canals, B.; Lacroix, C. *Phys. Rev. B* **2002**, *66*, 014422.

note that the degree of this DM interactions can be tuned by controlled synthetic methods, as evident from Figure 5. The fact that the DM interactions can be controlled has a potential in designing frustrated systems for various magnetic applications. It is noteworthy that the different degrees of distortion lead to significant differences in the magnetic properties of the Fe(II) Kagome compounds, a feature different from those of the Fe(III) jarosites with a d^5 ion. If such interactions with geometrical origin can be controlled in both integer spin and half-odd-integer spin Kagome system[17] requires further studies.

Conclusions

An organically templated iron(II) sulfate with a highly distorted Kagome lattice has been synthesized and characterized. The magnetic properties of this compound are distinctly different from those of other Fe(II) Kagome compounds possessing perfect or slightly distorted Kagome structures; the distorted Kagome compound prepared by us shows canted antiferromagnetism at low temperatures.

Acknowledgment. J.N.B. thanks CSIR, India, for a research fellowship. The authors thank Dr. S. K. Pati for helpful discussions.

Supporting Information Available: TGA curve, atomic coordinates, important bond distances and angles, hydrogen bonding interactions, and X-ray crystallographic information in CIF format for the structure determination of **III**. This material is available free of charge via the Internet at http://pubs.acs.org.

IC061457Y

(17) Pati, S. K.; Rao, C. N. R. *J. Chem. Phys*. **2005**, *123*, 234703.